



THE UNIVERSITY *of* EDINBURGH

Edinburgh Research Explorer

Optimization and Validation of a Human Ex Vivo Femoral Head Model for Preclinical Cartilage Research and Regenerative Therapies

Citation for published version:

Styczynska-Soczka, K, Amin, AK, Simpson, AHW & Hall, AC 2020, 'Optimization and Validation of a Human Ex Vivo Femoral Head Model for Preclinical Cartilage Research and Regenerative Therapies', *Cartilage*, vol. N/A, pp. 1-12. <https://doi.org/10.1177/1947603520934534>

Digital Object Identifier (DOI):

[10.1177/1947603520934534](https://doi.org/10.1177/1947603520934534)

Link:

[Link to publication record in Edinburgh Research Explorer](#)

Document Version:

Peer reviewed version

Published In:

Cartilage

General rights

Copyright for the publications made accessible via the Edinburgh Research Explorer is retained by the author(s) and / or other copyright owners and it is a condition of accessing these publications that users recognise and abide by the legal requirements associated with these rights.

Take down policy

The University of Edinburgh has made every reasonable effort to ensure that Edinburgh Research Explorer content complies with UK legislation. If you believe that the public display of this file breaches copyright please contact openaccess@ed.ac.uk providing details, and we will remove access to the work immediately and investigate your claim.



1
2 **Optimisation and validation of a human *ex vivo* femoral head**
3 **model for pre-clinical cartilage research and regenerative**
4 **therapies.**

5
6
7 Katarzyna Styczynska-Soczka,¹ Anish K. Amin,² A. Hamish W. Simpson,² Andrew C. Hall.¹

8
9 ¹Edinburgh Medical School: Biomedical Sciences,
10 Hugh Robson Building,
11 George Square,
12 Edinburgh EH8 9XD, U.K.

13
14 ²Department of Trauma and Orthopaedic Surgery,
15 Royal Infirmary of Edinburgh,
16 49 Little France Crescent,
17 Edinburgh EH16 4SA, U.K.
18

19 **Correspondence to:**

20
21 Dr Andrew C. Hall
22 Edinburgh Medical School: Biomedical Sciences,
23 University of Edinburgh,
24 Hugh Robson Building,
25 George Square,
26 Edinburgh EH8 9XD,
27 Scotland, U.K.
28 Phone + 44 (0)131 650 3263
29 FAX + 44 (0)131 650 2872
30 E.mail; a.hall@ed.ac.uk

31
32
33 **Key words:**

34 Femoral head, articular cartilage, chondrocytes, disuse atrophy, phenotype.
35

36
37
38
39
40
41
42
43
44
45
46
47
48
49
50
51
52
53
54
55
56
57
58
59
60

Abstract:

Objective. Articular cartilage is incapable of effective repair following injury or during osteoarthritis. While there have been developments in cartilage repair technologies, there is a need to advance biologically-relevant models for pre-clinical testing of biomaterial and regenerative therapies. This study describes conditions for the effective *ex vivo* culture of the whole human femoral head.

Design. Fresh, viable femoral heads were obtained from femoral neck fractures and cultured for up to 10wks in: (a) Dulbecco's modified Eagle's medium (DMEM); (b) DMEM+mixing; (c) DMEM+10% human serum (HS); (d) DMEM+10%HS+mixing. The viability, morphology, volume and density of fluorescently-labelled *in situ* chondrocytes and cartilage surface roughness were assessed by confocal microscopy. Cartilage histology was studied for glycosaminoglycan content using Alcian blue and collagen content using picosirius red.

Results. Chondrocyte viability remained at >95% in DMEM+10%HS. In DMEM alone, viability remained high for ~4wks then declined. For the other conditions, superficial zone chondrocyte viability fell to <35% at 10wks with deeper zones being relatively unaffected. In DMEM+10% HS at 10wks, the number of chondrocytes possessing cytoplasmic processes increased compared to DMEM ($p=0.017$). Alcian blue labelling decreased ($p=0.02$) and cartilage thinned ($p\leq 0.05$), however there was no change to surface roughness, chondrocyte density, chondrocyte volume, or picosirius red labelling ($p>0.05$).

Conclusions. In this *ex vivo* model, chondrocyte viability was maintained in human femoral heads for up to 10wks in culture, a novel finding not previously reported. This human model could prove invaluable for the exploration, development and assessment of pre-clinical cartilage repair and regenerative therapies.

61 **Introduction:**

62 Articular cartilage has very poor regenerative potential following injury and the repair tissue
63 formed is mechanically weak, and has a fibro-cartilageneous, rather than the resilient load-bearing
64 extracellular matrix (ECM) of hyaline cartilage¹. Furthermore, the native regeneration potential of
65 cartilage declines with age² and while fibro-cartilaginous repair can be observed to form within injured
66 hyaline cartilage, it is more evident when the injury has penetrated the sub-chondral bone.^{1,3} The
67 reasons for the production of mechanically-incompetent repair tissue are not well understood, and
68 clearly there is intense interest in developing more effective biomaterial and regenerative therapies
69 for cartilage repair. However, current models are not optimal and usually involve preparations
70 ranging from *in vitro* cultures of cells, through to osteochondral explants⁴ and *ex vivo* and *in vivo*
71 models of mainly animal (i.e. non-human) joints^{5,6}. The research and development of more effective
72 cartilage repair and regenerative therapies would be enhanced by the ability to pre-clinically evaluate
73 novel strategies in *ex vivo* physiological, tribological models of natural joints.

74 While there have been many detailed studies on explant and organ culture of animal
75 osteochondral tissue (e.g.⁷), few studies have conducted experiments directly on human tissue. The
76 limited studies using human cartilage for experimentation have obtained the material as discarded,
77 and frequently degenerate osteochondral tissue (e.g. during joint replacement surgery for
78 osteoarthritis)⁸. To test orthobiological treatments for human cartilage repair, the use of healthy
79 cartilage is essential. However, this source of material is difficult to obtain and relies on collaboration
80 between clinicians, theatre staff and research scientists. Whilst normal human cartilage may be
81 obtained from amputations, trauma victims or occasionally cadavers, such material is rarely available
82 for wider adoption into experimental human cartilage research. *Ex vivo* organ culture is becoming
83 increasingly important for basic and applied biomedical research because it is more representative
84 of normal cellular behaviour. However, obtaining a steady supply of viable human tissue which then
85 has to be cultured for weeks under aseptic conditions remains a challenging research area.

86 Femoral neck fractures are one of the most common surgically treated injuries in elderly
87 patients. The human femoral head is discarded during the surgery undertaken to treat femoral neck
88 fractures and is replaced with an artificial prosthesis. While this discarded femoral head is aged, it is
89 generally non-degenerate. We hypothesised that the human femoral head would be a viable source

90 of normal, non-degenerate articular cartilage suitable for pre-clinical cartilage research and
91 regenerative therapies. We were able to coordinate the timely, sterile collection and delivery of the
92 discarded human femoral head from the operating theatre to the laboratory. The aim of this study
93 was to optimise the culture conditions for fresh human femoral heads from femoral neck fractures to
94 permit viable long-term (10wk) culture.

95 **Methods**

96

97 *Human femoral heads*

98 Femoral heads were obtained with ethical permission (Tissue Governance, National Health
99 Service, Lothian) and patient consent from 15 patients (11 females, 4 males, mean age 75.5 (range
100 56-88)) undergoing hemi-arthroplasty or total hip replacement for femoral neck fracture (FNF).
101 Femoral heads were carefully removed intra-operatively by a qualified orthopaedic surgeon using a
102 corkscrew device and immediately placed into a sterile container with saline (0.9% w/v; 21°C) to
103 prevent chondrocyte death from drying⁹. Femoral heads were then transferred to a sterile container
104 with Dulbecco's Modified Eagle's Medium (DMEM) with D-glucose (25mM), L-Glutamine (4mM),
105 pyruvate (1mM), 100U/ml penicillin, 100µg/ml streptomycin, 2.5mg/ml amphotericin B (Sigma-
106 Aldrich, Irvine, UK) and 10µg/ml Fungin (InvivoGen, Toulouse, France) ready for transportation to
107 the laboratory with the femoral heads being available for experiments within 1-2hrs.

108

109 *Culture conditions*

110 Femoral heads were maintained in culture (37°C) in sealed single use sterile containers and
111 media changed every 3 days and the container replaced with every media change. Media volume
112 for each femoral head was ~50-60ml. Male femoral heads were larger than those of females (diam.
113 typically 6cm vs 4.5cm) and required larger culture containers. The femoral heads were cultured for
114 up to 10 weeks under the following conditions: (a) static culture in Dulbecco's modified Eagle's
115 medium (DMEM), (b) culture in DMEM with movement (DMEM+mixing), (c) as for (a) above +10%
116 normal human serum (HS, Merck, Feltham, U.K) and (d) as for (b) above +10% HS. A cavity was
117 carved in the cancellous bone of the femoral head for a magnetic stirring bar using bone trimmers
118 (Fig. 1). Containers were then placed on a magnetic mixer inside the incubator and stirring was
119 programmed for 1h, twice daily at ~1Hz. The rationale for studying the effects of movement was
120 based on our proof of concept bovine model where joint movement promoted chondrocyte viability⁷.

121

122 *Cartilage sampling, fluorescent labelling of in situ chondrocytes and confocal microscopy*

123 Full depth cartilage explants were harvested using 3 or 5mm diam. biopsy punches (Kai
124 Medical, Solingen, Germany) for weekly chondrocyte viability measurements. To minimise the
125 variability, explants were taken from random areas within the load-bearing parafoveal superior
126 region¹⁰ (Fig. 2). Cartilage samples were then incubated (1.5h;21°C) with CMFDA (5-
127 chloromethylfluorescein diacetate) cell tracker green and PI propidium iodide (12.5 and 10µM,
128 respectively; Invitrogen, Paisley, U.K.) to label living (green) and dead (red) cells respectively¹¹.
129 Explants were washed in phosphate-buffered saline (PBS; Invitrogen, Paisley, U.K.), fixed
130 (formaldehyde 4%v/v;30mins; Fisher, Leicestershire, U.K.) and imaged in three-dimensions by
131 confocal laser scanning microscopy (CLSM) using established methods¹².

132

133 *Measurements of chondrocyte viability, density, volume and morphology*

134 Confocal projected axial views were analysed using ImageJ/FIJI (National Institutes of
135 Health) and IMARIS software (Zurich, Switzerland) as described¹². Chondrocyte viability (% live
136 cells) was calculated as: the number of CMFDA-labelled cells/(number of CMFDA-labelled cells +
137 number of PI-labelled cells) in a given Region of Interest (ROI) volume. For chondrocyte density, the
138 total number of cells (CMFDA-labelled and PI-labelled) in the ROI volume were counted in IMARIS,
139 and results given as cells/µm³. Chondrocyte volumes were obtained using the IMARIS 'Surfaces'
140 algorithm. Volume calibration was performed using fluorescent microspheres (Polysciences,
141 Warrington, USA). Chondrocyte morphology was considered 'normal' if cells were visualised as
142 having a 'smooth' surface and elliptical/rounded shape. 'Abnormal' chondrocytes exhibited at least
143 one CMFDA-labelled cytoplasmic process ≥2µm long. Abnormal cells were counted manually and
144 divided by the total number of live cells in the field of view with results presented as the % abnormal
145 cells in the whole cell population within the ROI¹².

146

147 *Histology, cartilage thickness and surface roughness*

148 Explants were frozen (-80°C) in a freezing medium (1:1 Optimal temperature cutting
149 compound with 30% w/v sucrose in PBS for histology^{13,14}. The plugs were then cut into 40µm
150 sections and stained with Alcian blue (Vector Laboratories Ltd., Peterborough, U.K.) to label cartilage
151 glycosaminoglycans according to manufacturer's instructions. For picosirius red staining of

152 collagens, sections of 10 μ m thickness were first stained with haematoxylin for 8mins, then washed
153 3-4x in distilled water. This was followed by 1h incubation in 0.1% picosirius red (Direct Red 80,
154 Sigma-Aldrich, Irvine, U.K.) in picric acid (VWR International, Lutterworth, U.K.). Sections were
155 washed briefly 2x in 0.5% acetic acid, dehydrated (two washes in ethanol absolute followed by one
156 wash in xylene) and mounted in resinous mounting medium. Histological sections were imaged on
157 a Leica bright field microscope and analysed with ImageJ/FIJI software¹⁵. After converting the
158 images to greyscale 8-bit pixel depth, the same intensity threshold was set for each pair of sections
159 (week 0 vs week 10). The stained area above the threshold was measured and presented as a % of
160 the total sectional area. Cartilage thickness measurements were performed on the coronal sections
161 of cartilage using ImageJ/FIJI. For the surface roughness measurements, the ImageJ/FIJI Analyse
162 Stripes macro was used on the images of histologically-stained sections. Calculation of cartilage
163 surface roughness was based on the deviation from an idealized smooth cartilage surface, and
164 expressed as Rq (the root mean square (RMS) deviation) in μ m.

165

166 *Data presentation and statistical analysis*

167 Statistical analyses were performed using Graphpad Prism ver.8.2.1 (GraphPad Software,
168 La Jolla, U.S.A.). Data were presented as (N(n)), with (N) representing the number of independent
169 femoral heads and (n) the total number of replicates. Each data point presented on graphs and used
170 for statistical analyses was an average (\pm S.D. or S.E.M. as indicated) of the replicates taken from
171 each femoral head. Unless otherwise stated, paired Student's t-tests were used to compare
172 differences within pairs of treatment groups or time points, and ANOVA used to compare differences
173 across several groups. A significant difference was accepted when $p < 0.05$.

174 **Results**

175

176 *Cartilage grading and chondrocyte viability*

177 Femoral heads were macroscopically assessed using an established system¹⁶. For all
178 femoral heads considered suitable, the cartilage was grade 0 over >75% of the surface, with small
179 isolated grade 1 lesions in the parafoveal area (which were <25% of the surface area). The isolated
180 areas of grade 1 cartilage (mild surface fibrillation) were not studied and only cartilage of grade 0
181 was used.

182 Chondrocyte viability was assessed on day 1 and any femoral heads with a viability of <80%
183 were excluded. Out of a total of 24 femoral heads received, five were excluded due to low initial
184 chondrocyte viability and a further four were also excluded as they developed infection during
185 subsequent culture. In the remaining 15 femoral heads, the cell viability was 95.3±5.3%
186 (N(n)=15(60)) on Day 1. Chondrocyte viability in femoral heads cultured under static conditions in
187 DMEM remained high (>90%) for ~4wks but decreased to 44.0±22.3% by week 10 (N(n)=4(16), one-
188 way ANOVA, post-test for trend, $p=0.045$, Fig. 3A). This decrease in cell viability was accelerated
189 with movement of the femoral head and stirring of the media with virtually no viable cells by week 6
190 (two-way ANOVA; $p=0.0099$, Fig. 3A). The addition of 10% HS to DMEM maintained chondrocyte
191 viability at >90% to week 10 under static femoral head culture conditions (Fig. 3B) but did not
192 significantly improve the viability in femoral head cultures with movement/stirring over 10 weeks.

193 CLSM permits three-dimensional imaging and quantitative analyses of chondrocyte viability
194 within the full depth of cartilage¹⁷. To assess if chondrocytes within any zone were more sensitive
195 during culture, chondrocyte viability was determined as a function of depth from the articular surface.
196 We compared the percentage cell viability within the different zones (SZ, MZ, DZ) in coronal sections
197 of articular cartilage at week 10 compared with baseline (week 0). There was a decrease in the SZ
198 viability in both culture conditions (DMEM only, and DMEM+mixing; ($p=0.0425$ and $p=0.016$
199 respectively; Fig. 4A)) with relative preservation of cell viability in deeper cartilage zones (Fig. 4B).
200 This suggest that SZ chondrocytes were far more sensitive to the culture conditions compared to the
201 cells in the deeper zones. Thus, although there were few living SZ cells remaining after 10wks, a
202 substantial portion of chondrocytes in the other zones were still viable.

203

204 *Chondrocyte morphology*

205 In fresh explants of macroscopically non-degenerate femoral head cartilage, a small
206 population ($8.0\pm 1.5\%$ ($N(n)=4(8)$)) of cells in the SZ ($\sim 100\mu\text{m}$ from the surface) demonstrated one or
207 more cytoplasmic processes (Fig 5. A,B). During femoral head culture in DMEM, there appeared to
208 be an increase in the % of cells with processes (to $15\pm 5.3\%$ by week 6, $N(n)=4(16)$) and ($16\pm 6.4\%$
209 by week 10 $N(n)=4(16)$) however these changes were not significantly different compared to week
210 0 (ANOVA; $p>0.05$). In contrast, in the presence of HS, the % of chondrocytes with processes
211 increased to $31\pm 9.3\%$ by week 6 ($p=0.008$; $N(n)=3(12)$) and $37\pm 7.1\%$ by week 10
212 ($p=0.002$; $N(n)=3(12)$) compared to week 0 (Fig. 5B). By week 10, there were significantly more (by
213 >2 -fold; $p=0.017$) chondrocytes with cytoplasmic processes when femoral heads were cultured in
214 DMEM+HS compared to DMEM alone (Fig. 5B).

215

216 *Extracellular matrix composition*

217 To evaluate whether extracellular matrix composition changed during culture, two histological
218 stainings were performed on cartilage samples (week 0 and week 10) and analysed semi-
219 quantitatively. There was a general trend of decreasing GAG staining using Alcian blue¹⁸ under all
220 culture conditions, but in DMEM+HS chondrocyte viability was significantly higher (Fig. 6A). In these
221 cultures $50.0\pm 2.86\%$ ($N(n)=3(6)$) of the section area was stained with Alcian blue at week 0. This
222 decreased to $17.0\pm 13.8\%$ by week 10 ($N(n)=3(6)$; $p=0.028$). The total collagen stained with
223 picosirius red did not show any significant difference between DMEM and DMEM+HS samples at
224 week 0 and week 10 ($30\pm 5\%$ vs $42\pm 22\%$, $N(n)=11(22)$; $p=0.09$). These results suggest a significant
225 loss of GAGs but no change to the total collagen content of femoral head cartilage during this culture
226 period.

227

228 *Cartilage thickness and surface roughness*

229 In parallel with the loss of GAGs, cartilage thickness was reduced after 10wks in culture (Fig.
230 6B). In DMEM cultures, it decreased from $3808\pm 425\mu\text{m}$ to $2828\pm 542\mu\text{m}$ ($p=0.05$; $N(n)=4(22)$). In the
231 DMEM+mixing culture it declined from $4226\pm 418\mu\text{m}$ to $2703\pm 720\mu\text{m}$ ($p=0.02$; $N(n)=4(15)$), and in

232 DMEM+10% human serum it decreased from $3377\pm360\mu\text{m}$ to $2349\pm160\mu\text{m}$ ($p=0.02$;N(n)=3(22)).
233 Articular surface roughness assessed on the same femoral heads at week 0 and week 10 was not
234 significantly different ($13\pm0.6\mu\text{m}$ and $15\pm0.7\mu\text{m}$ respectively ($p=0.55$;N(n)=9(9);Fig. 7A)).

235

236 *Chondrocyte density and volume*

237 There was no difference in cell density for all the samples at week 0 (9971 ± 2389 cells/mm³
238 N(n)=15(60)) compared with week 10 (11256 ± 3305 cells/mm³ ($p=0.01$;N(n)=15(60));Fig 7B)). *In situ*
239 chondrocyte volume was also analysed as it correlates with the progression of cartilage
240 degeneration, however, there was no difference ($p=0.22$) between the cell volumes of chondrocytes
241 on day 0 ($423\pm49\mu\text{m}^3$, N(n)=15(60) and week 10 ($441\pm48\mu\text{m}^3$, N(n)=15(60);Fig. 7C)).

242

243

244

245 **Discussion.**

246 We have established culture conditions which maintain chondrocyte viability during *ex vivo*
247 culture of human femoral heads for 10 weeks by supplementing standard culture medium with 10%
248 normal human serum. We have identified an excellent and reliable source of viable, non-degenerate
249 human articular cartilage ideal for *ex vivo* experimentation. Previously, we have investigated the
250 microscopic effects of mechanical and other forms of injury on human articular cartilage^{9,19}. However
251 material was obtained from tissue discarded during knee replacement for osteoarthritis and the yield
252 of non-degenerate tissue was often low. This was because the majority of the tissue was
253 osteoarthritic with loss of superficial zone cells, even if macroscopically the tissue may have
254 appeared non-degenerate. In contrast, the cartilage of the femoral head discarded after femoral neck
255 fracture was in most cases non-degenerate and our experiments have confirmed the presence of
256 viable cartilage tissue that is macroscopically and microscopically ideally suited for investigating
257 cartilage repair and regeneration. Due to the excellent chondrocyte viability throughout culture, the
258 model may also allow *ex vivo* validation of an optimal combination of cells, growth factors and
259 scaffolds that lead to the formation of repair tissue resembling the desirable hyaline articular cartilage
260 at the microscopic level.

261 Current knowledge of the microscopic quality of cartilage repair tissue in humans is based
262 on histological assessment of opportunistic biopsy specimens retrieved during 'second look'
263 arthroscopy (keyhole surgery). While these specimens have provided valuable insight into the quality
264 of cartilage repair, with so called 'hyaline-like' composition, the information is limited by small
265 numbers of specimens, distortion of the tissue during biopsy, variability in the site/size of biopsies
266 and heterogeneity of the study sample. The lack of a non-invasive method of evaluating the
267 microscopic characteristics of the quality of the cartilage repair tissue has also been recognized as
268 a major problem limiting advances in cartilage repair and regenerative techniques by the
269 International Cartilage Repair Society (ICRS)²⁰. Modern imaging techniques (e.g. CLSM) allow
270 microscopic examination of articular cartilage by optically sectioning the tissue. We believe that the
271 significantly easier access to normal, human cartilage *ex vivo* will help overcome the problems
272 associated with *in vivo* biopsy, and allow detailed quantitative microscopic assessment and

273 optimisation of the quality of cartilage repair. The proposed model will significantly enhance our
274 ability to test a wide range of pre-clinical therapeutic cartilage repair and regenerative strategies
275 directly in human tissue so that the best candidate therapies can be identified for subsequent clinical
276 study.

277 In our model, the large area of grade 0 cartilage (Fig. 1) permitted multiple samples to be
278 taken either at a single time point, or a smaller number over a longer time course. A gap between
279 samples was retained so that cutting trauma using the biopsy punch²¹ did not influence neighbouring
280 samples. Furthermore, if cartilage wells were to contain biological models for testing, then it would
281 be possible for the full depth sample to be 'scooped' out using a fine scalpel blade. Chondrocyte
282 viability in both axial and coronal projections was initially high for all samples (Fig. 3A). There was
283 no change in viability during DMEM+HS culture, suggesting that taking multiple cartilage plugs over
284 the 10wk period did not adversely affect the viability of the surrounding cartilage. It should be noted
285 that if serum (HS) was used, then it must be heat-treated because it contains enzymes that digest
286 the DNA of dead cells leading to an under-estimation of the dead cell population^{22,23}.

287 Femoral head culture in DMEM maintained chondrocyte viability for ~4wks after which there
288 was an increase in chondrocyte death (Fig. 3A). With mixing, viability decreased progressively after
289 the start of the culture, such that by week 10 there were virtually no remaining viable cells.
290 Furthermore, cell death started in the SZ so that after 10wks, all these chondrocytes were dead
291 whereas those in the deeper zones were still viable (Fig. 4). This suggests that there are factors in
292 bone supporting chondrocyte viability in the superficial zone which were washed out during media
293 changes. The importance of bone in cultures of bovine cartilage has been reported previously as SZ
294 chondrocyte viability was maintained in cartilage cultures when bone was present either when
295 attached to the explants or in co-culture²⁴. This was in contrast to deep zone chondrocytes which
296 survived, and the relative viability of these chondrocytes within the femoral head cartilage of our
297 elderly patients (Fig. 4) parallels the long-term (~25yr) survival of DZ chondrocytes in osteochondral
298 allografts used for the treatment of focal post-traumatic defects in young individuals²⁵. It is possible
299 that these chondrocytes are well adapted to this relatively hostile environment for example
300 chondrocytes in the DZ utilise different membrane transport systems for the regulation of intracellular
301 acidity compared to cells in the SZ²⁶. The addition of HS in the mixed DMEM condition provided

302 some protection for SZ chondrocytes as cell viability by week 10 was 35% (Fig. 3B). However, if
303 there was no mixing and HS was present, there was complete chondrocyte protection suggesting
304 that serum was protecting the cells which were vulnerable during the latter stages of the culture.
305 While the cross-talk between subchondral bone and cartilage has received considerable attention²⁷
306 the factor(s) released from bone and/or present in the serum which promote chondrocyte viability
307 are unclear, with TGF β , IGF-1 and BMP being implicated²⁸.

308 Visualisation of fluorescently-labelled *in situ* chondrocytes revealed the classical morphology
309 of elliptical cells in the SZ with the more spheroidal forms in the deeper zones (Fig. 4)¹². In grade 0
310 cartilage in axial projections, a small proportion (~8%) of the SZ cells (within ~100 μ m depth).
311 exhibited cytoplasmic processes. Of interest was that after 10wks of culture in DMEM+HS, there
312 was a significant (>4-fold) increase in the % of cells exhibiting processes (Fig. 5A). At week 10,
313 significantly (by >2-fold) more chondrocytes demonstrated a cytoplasmic process when HS was
314 present compared to culture in DMEM alone. However, in the DMEM+HS condition, chondrocyte
315 viability and density did not change during culture (Figs. 3B & 7B respectively), whereas in DMEM
316 alone viability had decreased by ~50% (Fig. 3A) but abnormal chondrocytes were still present (Fig.
317 5B). The changes to chondrocyte shape might be related to the properties of the ECM. In healthy
318 cartilage, the pore size of the PG network is ~3nm whereas that for collagen is ~100nm and thus the
319 PGs will regulate cartilage permeability and solute diffusivity²⁹. GAG loss during unloading will
320 increase matrix permeability and thus potent growth factors etc., in serum will start to penetrate and
321 act particularly on SZ chondrocytes which are normally shielded by the tight matrix. The development
322 of processes and subsequent abnormal morphology of chondrocytes is a feature associated with de-
323 differentiation to a fibroblastic phenotype^{30,31} and has been observed in osteoarthritic tibial and
324 femoral head cartilage^{17,32,33}. A change in phenotype is characterised by decreased hyaline cartilage-
325 specific collagen type II and aggrecan production, and an increase in collagen type I production. It
326 would be of particular interest to determine if physiological levels of loading could reverse some of
327 these changes and protect the chondrocyte phenotype and promote the production of a hyaline
328 cartilage¹⁷.

329 There was no evidence of chondrocyte clustering³⁴ under any of the experimental conditions.
330 Nomura et al.³⁵ did not observe changes to chondrocyte morphology in mice subjected to hindlimb

331 unloading when cartilage was studied by histology. This might appear to conflict with the changes to
332 chondrocyte morphology reported here. However the detection of the fine cytoplasmic process is not
333 possible with their histological techniques as they involve tissue shrinkage³⁶ and high resolution
334 imaging of unperturbed *in situ* chondrocytes is essential for the visualisation of the processes^{17,31}.

335 It might be considered that a limitation in our study was that no mechanical load was applied
336 to the femoral heads. However this revealed that after 10wks there were features of the cartilage
337 ECM and *in situ* chondrocytes which bear similarities to the changes observed with both *in vivo* and
338 *in vitro* cartilage disuse atrophy. Alcian blue staining reflecting GAG content was decreased (Fig.
339 6A,C). This was not significant in the DMEM and DMEM+mixing conditions when there was
340 substantial chondrocyte death (~50% and 100% respectively). However, interestingly, the decrease
341 was significant in the DMEM+HS condition (Fig.6A) when cell viability was high (>95%). This
342 suggests that there was an active chondrocyte-driven process mediating reduced GAG levels³⁷.
343 GAG loss would probably account for the cartilage thinning (Fig. 6B), reported by others using animal
344 joint immobilisation models³⁵. GAG loss did not however, affect surface roughness (Fig. 7A) which
345 is in contrast to the changes occurring in OA, where GAG levels decrease and surface roughness
346 and cartilage fibrillation increase²⁸. Palmoski *et al.*³⁸ noted a similar decrease in PG staining in
347 healthy adult dogs after ~6 days of immobilisation and by 8wks there was a 30-50% reduction in
348 cartilage thickness with an almost complete loss of PG. In human joints immobilised as a result of
349 ankle fracture, there was a 6.6% loss of cartilage thickness over 7wks following fracture³⁹. The loss
350 of GAGs is thought to be due to a reduction in synthesis as well as the stimulation of chondrocyte
351 degradative enzyme (MMP-13, ADAMTS5) activity^{35,37} from a mechano-adaptive response to
352 reduced load. Mechanical loading of joints is a key parameter for maintaining the differentiated,
353 rounded, chondrocyte phenotype^{40,41}. Recent studies implicate an essential role for the
354 mechanosensitive ion channel Transient Receptor Potential Vanilloid 4 (TRPV4) in the signal
355 transduction pathway. Inhibiting TRPV4 prevents loading-mediated increases in matrix synthesis,
356 whereas activating TRPV4 in the absence of loading increases matrix synthesis in a manner
357 analogous to loading⁴².

358 While there were changes to GAG labelling, there was no change to picosirius red labelling
359 suggesting the cartilage collagen content remained unaltered throughout culture. While picosirius

360 red does not discriminate between the collagen types⁴³ it is possible that there were changes to
361 collagen metabolism and/or its organisation. For example, while total collagen content might not
362 have change significantly, it is possible that there was a decrease in the collagen type II : type I ratio
363 reflecting chondrocyte de-differentiation. In addition, changes to collagen fibre distribution/orientation
364 could be evident, and future studies utilising polarized light microscopy would be worth pursuing. A
365 small decrease in collagen cross-linking which recovers after re-mobilisation has been reported⁴⁴
366 and the immobilisation of rabbit knee joint leads to a partial shift in the density of collagen
367 composition from type II to type I⁴⁵. However, in human cartilage, there is negligible/minimal collagen
368 turnover over the lifetime in a healthy joint⁴⁶.

369 There was no change to the volume of *in situ* chondrocytes following 10wks culture in
370 DMEM+HS (Fig. 7C). It is likely that with the loss of GAGs, interstitial osmolarity of the matrix would
371 decrease, leading to hypo-osmolarity and cell swelling. However *in situ* chondrocytes possess
372 effective volume-regulatory channels and transporters^{47,48} and over a long time period, despite the
373 change in osmolarity, these mechanisms could compensate leading to no volume change. This
374 phenomenon (termed iso-volumetric volume regulation (IVR)) has been described in various cell
375 types including chondrocytes⁴⁹. The lack of chondrocyte swelling is in contrast to that observed in
376 osteoarthritic cartilage where increased chondrocyte volume/hypertrophy has been reported^{17,50}.

377 This study described the first successful *ex vivo* culture of a large human joint. *In situ*
378 chondrocyte viability remained high in DMEM+HS, however it decreased under the other conditions
379 tested. Although chondrocyte viability was optimal, there were changes to the matrix (cartilage
380 thinning, GAG loss, no change to collagen or surface roughness) and chondrocytes (development
381 of cytoplasmic processes, no change to volume or density). This pre-clinical model may be an
382 invaluable addition for the assessment of human cartilage repair therapies and may replace some
383 animal studies.

384

385 **Acknowledgements.**

386 We thank Ms F. Stewart for excellent assistance with the provision of the femoral heads, Dr
387 A. Kubasik-Thayil at the IMPACT imaging facility in the Centre for expert assistance with confocal
388 imaging, and Ms A. Luczak for assistance with histology.

389

390 **Role of the Funding Source.**

391 This work was supported by a project grant from the Chief Scientist's Office (Scotland)
392 TCS/18/01.

393

394 **Author Contributions.**

395 Study concept and design; Amin, Simpson, Hall. Acquisition of data; Styczynska-Soczka.
396 Analysis and interpretation of data; Styczynska-Soczka, Amin, Simpson, Hall. Manuscript
397 preparation; Styczynska-Soczka, Amin, Simpson, Hall.

398

399 **Conflict of Interest.**

400

401 The authors have no conflicts of interest to declare.

402 **References.**

403

404 1. Hunziker EB, Lippuner K, Keel MJB, Shintani N. An educational review of cartilage repair:
405 precepts & practice - myths & misconceptions - progress & prospects. *Osteoarthritis and Cartilage*
406 2015;23:334-350 <http://dx.doi.org/10.1016/j.joca.2014.12.011>

407

408 2. Brittberg M, Gomoll AH, Canseco JA, Far J, Lind M, Hui J. Cartilage repair in the degenerative
409 ageing knee. *Acta Orthopaedica* 2016;87:sup363, 26-38, DOI: 10.1080/17453674.2016.1265877

410

411 3. Simon TM, Aberman HM. Cartilage regeneration and repair testing in a surrogate large animal
412 model. *Tissue Eng Part B Rev* 2010;16:65-79. DOI: 10.1089/ten.TEB.2009.0304.

413

414 4. Maglio M, Tschon M, Sicuro L, Lolli R, Fini M. Osteochondral tissue cultures: between limits and
415 sparks, the next step for advanced in vitro models. *J Cell Physiol* 2018;234:5420-5435. DOI:
416 10.1002/jcp.27457

417

418 5. Elson KM, Fox N, Tipper JL, Kirkham J, Hall RM, Fisher J, *et al*, Non-destructive monitoring of
419 viability in an ex vivo organ culture model of osteochondral tissue. *Europ Cells Mat* 2015;29:356-
420 369. DOI: 10.22203/eCM.v029a27

421

422 6. Cope PJ, Ourradi K, Li Y, Sharif M. Models of osteoarthritis: the good, the bad and the
423 promising. *Osteoarthritis and Cartilage* 2019;27:230-239.
424 <https://doi.org/10.1016/j.joca.2018.09.016>

425

426 7. Lin Y-C, Hall AC, Simpson AHRW. A novel joint organ culture model for evaluation of static and
427 dynamic load on articular cartilage. *Bone & Joint Research* 2018;7(3):205-212. DOI:10.1302/2046-
428 3758.73BJR-2017-0320

429

- 430 8. Geurts J, Juric D, Müller M, Schären S, Netzer C. Novel ex vivo human osteochondral explant
431 model of knee and spine osteoarthritis enables assessment of inflammatory and drug treatment
432 responses. *Int J Mol Sci* 2018;19:1314. DOI: 10.3390/ijms19051314
433
- 434 9. Paterson SI, Amin AK, Hall AC. Airflow accelerates bovine and human articular cartilage drying
435 and chondrocyte death. *Osteoarthritis and Cartilage* 2015;23:257-265. DOI:
436 10.1016/j.joca.2014.10.004.
437
- 438 10. Greenwald AS, Haynes DW. Weight-bearing areas in the human hip joint. *J Bone Jt Surg (Br)*.
439 1972;54(1):157-63.
440
- 441 11. Amin AK, Bush PG, Huntley JS, Simpson AHW, Hall AC. Osmolarity influences chondrocyte
442 death in wounded articular cartilage. *J Bone Jt Surg (Amer)* 2008;90:1531-1542. DOI:
443 10.2106/JBJS.G.00857
444
- 445 12. Karim A, Amin AK, Hall AC. The clustering and morphology of chondrocytes in normal and
446 mildly-degenerate human femoral head cartilage studied by confocal laser scanning microscopy. *J*
447 *Anatomy* 2018;232(4):686-698. DOI: 10.1111/joa.12768.
448
- 449 13. Hyllested JL, Veje K, Ostergaard K. Histochemical studies of the extracellular matrix of human
450 articular cartilage - A review. *Osteoarthritis and Cartilage* 2002;10:333-343.
451 <https://doi.org/10.1053/joca.2002.0519>
452
- 453 14. Schmitz N, Laverty S, Kraus VB, Aigner T. Basic methods in histopathology of joint tissues.
454 *Osteoarthritis Cartilage* 2010;18:S113-S116. <https://doi.org/10.1016/j.joca.2010.05.026>
455
- 456 15. Crowe AR, Yue W. Semi-quantitative determination of protein expression using
457 immunohistochemistry staining and analysis: An integrated protocol. *Bio Protoc* 2019;9(24) pii:
458 e3465. DOI: 10.21769/BioProtoc.3465.

459

460 16. Pritzker KPH, Gay S, Jimenez SA, Ostergaard K, Peletier J–P, Revell PA, *et al* (2006).

461 Osteoarthritis cartilage histopathology: grading and staging. *Osteoarthritis and Cartilage*

462 2006;13:13-29. DOI:10.1016/j.joca.2005.07.014

463

464 17. Bush PG, Hall AC. The volume and morphology of chondrocytes within non-degenerate and
465 degenerate human articular cartilage. *Osteoarthritis and Cartilage* 2003;11(4):242-251.

466 DOI:10.1016/s1063-4584(02)00369-2

467

468 18. Fisher M, Solursh M. Glycosaminoglycan localisation and role in maintenance of tissue spaces
469 in the early chick embryo. *J Embryol Exp Morphol* 1977;42:195-207.

470

471 19. Amin AK, Huntley JS, Patton JT, Brenkel IJ, Simpson AHRW, Hall AC. Hyperosmolarity

472 protects chondrocytes from mechanical injury in human articular cartilage. *J Bone Joint Surg [Br]*

473 2011;93-B:277-84. Doi: 10.1302/0301-620X.93B2.24977.

474

475 20. Hoemann C, Kandel R, Roberts S, Saris DB, Creemers L, Mainil-Varlet P *et al*. International

476 Cartilage Repair Society (ICRS) Recommended Guidelines for Histological Endpoints for Cartilage

477 Repair Studies in Animal Models and Clinical Trials. *Cartilage* 2011;2(2);153-72.

478 Doi:10.1177/1947603510397535.

479

480 21. Huntley JS, McBirnie JM, Simpson AH, Hall AC. Cutting-edge design to improve cell viability in
481 osteochondral grafts. *Osteoarthritis and Cartilage* 2005;13:665-671. DOI:

482 10.1016/j.joca.2005.04.007

483

484 22. Zhou S, Cui Z, Urban JPG. Dead cell counts during serum cultivation are under-estimated by
485 the fluorescent live/dead assay. *Biotechnol J* 2011;6(5):513-518. DOI: 10.1002/biot.201000254.

486

- 487 23. Karim A, Hall AC. Hyperosmolarity normalizes serum-induced changes to chondrocyte
488 properties in a model of cartilage injury. *Europ Cells Mat* 2016;31:205-220. DOI:
489 10.22203/ecm.v031a14
490
- 491 24. Amin AK, Huntley JS, Simpson AHW, Hall AC. Chondrocyte survival in articular cartilage: the
492 influence of subchondral bone in a bovine model. *J Bone Jt Surg (Br)* 2009;91-B:691-699. DOI:
493 10.1302/0301-620X.91B5.21544
494
- 495 25. Gross AE, Kim W, Las Heras F, Backstein D, Safir O, Pritzker KP. Fresh osteochondral
496 allografts for posttraumatic knee defects: long-term followup. *Clin Orthop Relat Res*
497 2008;466(8):1863-70. DOI: 10.1007/s11999-008-0282-8.
498
- 499 26. Simpkin VL, Murray DH, Hall AP, Hall AC. Bicarbonate-dependent pH_i regulation by
500 chondrocytes within the superficial zone of bovine articular cartilage. *J Cell Physiol* 2007;212(3),
501 600-609. DOI: 10.1002/jcp.21054
502
- 503 27. Goldring SR, Goldring MB. Changes in the osteochondral unit during osteoarthritis: structure,
504 function and cartilage-bone crosstalk. *Nat Rev Rheumatol* 2016;12(11):632-644.
505 DOI: 10.1038/nrrheum.2016.148.
506
- 507 28. Loeser RF, Goldring SR, Scanzello CR, Goldring MB. Osteoarthritis: A disease of the joint as
508 an organ. *Arth Rheum* 2012;64(6):1697–1707. DOI:10.1002/art.34453
509
- 510 29. Graham BT, Wright AD, Burris DL, Axe MJ, Rasis LW, Price C. Quantification of solute
511 diffusivity in osteoarthritic human femoral head cartilage using correlation spectroscopy. *J Orthop*
512 *Res* 2018;36:3256-3267. DOI: 10.1002/jor.24138
513

- 514 30. Graceffa V, Vinatier C, Guicheux J, Stoddart M, Alini M, Zeugolis DI. Chasing chimeras – the
515 elusive stable chondrogenic phenotype. *Biomaterials* 2019;192:199–225.
516 <https://doi.org/10.1016/j.biomaterials.2018.11.014>
517
- 518 31. Hall AC. The role of chondrocyte morphology and volume in controlling phenotype –
519 implications for osteoarthritis, cartilage repair and cartilage engineering. *Curr Top Rheumatol*
520 2019;21:38 [https://doi: 10.1007/s11926-019-0837-6](https://doi.org/10.1007/s11926-019-0837-6)
521
- 522 32. Holloway I, Kayser M, Lee DA, Bader DL, Bentley G, Knight MM. Increased presence of cells
523 with multiple elongated processes in osteoarthritic femoral head cartilage. *Osteoarthritis and*
524 *Cartilage* 2004;12:17–24. <https://doi.org/10.1016/j.joca.2003.09.001>.
525
- 526 33. Tesche F, Miosge N. New aspects of the pathogenesis of osteoarthritis: the role of fibroblast-
527 like chondrocytes in late stages of the disease. *Histol Histopathol* 2005;20:329–37. DOI:
528 10.14670/HH-20.329
529
- 530 34. Lotz MK, Otsuki S, Grogan SP, Sah R, Terkeltaub R, D'Lima D. Cartilage cell clusters. *Arthritis*
531 *Rheum* 2010;62:2206–2218. DOI: 10.1002/art.27528.
532
- 533 35. Nomura M, Sakitani N, Iwaawa H, Kohara Y, Takano S, Wakimoto Y, *et al.* Thinning of articular
534 cartilage after joint unloading or immobilization. An experimental investigation of the pathogenesis
535 in mice. *Osteoarthritis and Cartilage* 2017;25:727-736. DOI: 10.1002/jor.1100070305
536
- 537 36. Loqman MY, Bush PG, Farquharson C, Hall AC. A cell shrinkage artefact in growth plate
538 chondrocytes with common fixative solutions: importance of fixative osmolarity for maintaining
539 morphology. *Eur. Cell. Mater.* 2010;19:214-27. DOI:10.22203/ecm.v019a21
540
- 541 37. Grumbles RM, Howell DS, Howard GA, Roos BA, Setton LA, Mow VC, *et al.*, Cartilage
542 metalloproteinases in disuse atrophy. *J Rheumatol Supp* 1995;43:46-148.

543

544 38. Palmoski M, Perricone E, Brandt KD. Development and reversal of a proteoglycan aggregation
545 defect in normal canine knee cartilage after immobilization. *Arth Rheum* 1979;22:508–517.

546

547 39. Behrens F, Kraft EL, Oegema TR Jr. Biochemical changes in articular cartilage after joint
548 immobilization by casting or external fixation. *J Orthop Res* 1989;7(3):335-343. DOI:
549 10.1002/jor.1100070305

550

551 40. Sanchez-Adams J, Leddy HA, McNulty AL, O’Conor CJ, Guilak F. The mechanobiology of
552 articular cartilage: bearing the burden of osteoarthritis. *Curr Rheumatol Rep* 2014;16(10):451.
553 DOI: 10.1007/s11926-014-0451-6.

554

555 41. Wuest SL, Calio M, Wernas T, Tanner S, Giger-lange C, Wyss F, *et al.* Influence of
556 mechanical unloading on articular chondrocyte dedifferentiation. *Int J Molecular Sciences*
557 2018;19(5). DOI: 10.3390/ijms19051289

558

559 42. O’Conor CJ, Leddy HA, Benefield HC, Liedtke WB & Guilak F. TRPV4-mediated
560 mechanotransduction regulates the metabolic response of chondrocytes to dynamic loading. *Proc*
561 *Natl Acad Sci USA* 2014;111:1316-1321. DOI: 10.1073/pnas.1319569111

562

563 43. Lattouf R, Younes R, Lutomski D, Naaman N, Godeau, G., Senni, K, *et al.* Picrosirius red
564 staining: A useful tool to appraise collagen networks in normal and pathological tissues. *J*
565 *Histochem Cytochem* 2014;62(10):751–758. DOI: 10.1369/0022155414545787

566

567 44. Haapala J, Arokoski JP, Hyttinen MM, Lammi M, Tammi M, Kovanen V, *et al.* Remobilization
568 does not fully restore immobilization induced articular cartilage atrophy. *Clin Orthop Relat Res*
569 1999;362:218–229.

570

- 571 45. Aldahmash AM, El Fouhil AF, Mohamed RA, Ahmed AM, Atteya M, Al Sharawy SA, *et al.*
572 Collagen types I and II distribution: a relevant indicator for the functional properties of articular
573 cartilage in immobilised and remobilised rabbit knee joints. *Folia Morphol* 2015;74(2):169–175.
574 DOI: 10.5603/FM.2015.0027.
- 575
- 576 46. Heinemeier KM, Schjerling P, Heinemeier J, Møller MB, Krogsgaard MR, Grum-Schwensen T,
577 *et al.* Radiocarbon dating reveals minimal collagen turnover in both healthy and osteoarthritic
578 human cartilage. *Sci Transl Med* 2016;8:346ra90. DOI: 10.1126/scitranslmed.aad8335.
- 579
- 580 47. Bush PG, Hall AC. Regulatory volume decrease (RVD) by isolated and in situ bovine articular
581 chondrocytes. *J Cell Physiol* 2001;187:304-14. DOI: 10.1002/jcp.1077
- 582
- 583 48. Lewis R, Feetham C, Barrett-Jolley R. Cell volume control in chondrocytes. *Cell Physiol*
584 *Biochem* 2011;28:1111–22. DOI: 10.1159/000335847.
- 585
- 586 49. Wang Z, Irianto J, Kazun S, Wang W, Knight MM. The rate of hypo-osmotic challenge
587 influences regulatory volume decrease (RVD) and mechanical properties of articular chondrocytes.
588 *Osteoarthritis and Cartilage* 2015;23:289-299. <http://dx.doi.org/10.1016/j.joca.2014.11.003>
- 589
- 590 50. Gratal P, Mediero A, Sánchez-Pernaute O, Prieto-Potin I, Lamuedra A, Herrero-Beaumont, G,
591 *et al.* Chondrocyte enlargement is a marker of osteoarthritis severity. *Osteoarthritis and Cartilage*
592 2019;27(8);1229-1234. DOI: 10.1016/j.joca.2019.04.013.
- 593
- 594

595

596 **Figure Legends.**

597

598 **Figure 1.** The cavity produced in the cancellous bone of the human femoral head to accommodate
599 the magnetic bar for stirring culture experiments.

600

601 **Figure 2. Localisation of the cartilage area on human femoral heads used for sampling. (A)**
602 Lateral view of the femoral head, fovea (F) on the upper left, **(B)** Top view of the femoral head, **(C)**
603 Femoral head with biopsy explants taken from within the specified zone. Scale bar represents 25mm.

604

605 **Figure 3. The viability of *in situ* human chondrocytes within femoral head cartilage cultured**
606 **under various conditions. (A)** DMEM N(n)=4(16); DMEM + mixing (N(n)=3(12)). **(B)** DMEM +
607 normal human serum (HS); (N(n)=3(12)), DMEM + mixing + human serum (N(n)=2(8)); error bars
608 represent S.E.M. (or S.D. for N=2). **(C)** Representative images of viability staining (CMFDA green –
609 live cells, PI red – dead cells) at week 10 for DMEM, DMEM + 10% human serum and DMEM +
610 mixing; scale bars represent 100µm.

611

612 **Figure 4. Viability of chondrocytes in various zones after 10 weeks of femoral head culture**
613 **(A)** Comparison of chondrocyte viability in the whole thickness vs superficial zone at week 10 of
614 culture. DMEM N(n)=4(16), * $p=0.0425$, DMEM + mixing, N(n)=3(12), * $p=0.016$ (data shown as mean
615 \pm S.E.M.). **(B)** Representative coronal images of labelled chondrocytes within cartilage sections
616 cultured in DMEM on day 0 (left panel), and after 10 weeks of culture in DMEM + mixing + HS on
617 week 10 (right panel). The scale bars represent 100µm.

618

619 **Figure 5. Changes to the morphology of *in situ* femoral head chondrocytes during culture.**
620 Panel **(A)** shows the % of cells with cytoplasmic processes at three time points (weeks 0, 6 and 10)
621 in cultures with DMEM (N(n) = 4(16)) and DMEM + human normal human serum (HS) (N(n) = 3(12)).
622 (Data shown as mean \pm S.D.). Panel **(B)** shows representative images of cell stained with CMFDA

623 cell tracker green to visualise chondrocyte morphology, and propidium iodide (PI) red to identify dead
624 cells. The top row of images is from DMEM cultures, (left to right panels for weeks 0, 6 and 10
625 respectively), the bottom row of images for DMEM + human serum (left to right panels for weeks 0,
626 6 and 10 respectively. Note examples of chondrocytes with cellular processes indicated by white
627 arrowheads. The scale bar represents 100µm.

628

629 **Figure 6. Histology of femoral head cartilage with time in culture. (A)** GAG content in various
630 culture conditions, (a) DMEM N(n)=4(8), (b) DMEM + mixing N(n)=4(8), (c) DMEM + 10% human
631 serum N(n)=3(6), * $p=0.028$. **(B)** Cartilage thickness in various culture conditions, (a) DMEM
632 N(n)=4(24), (b) DMEM + mixing N(n)=4(24), (c) DMEM + 10% human serum N(n)=3(18), ($p=0.05$;
633 $p=0.02$; $p=0.02$ respectively). (Data shown as mean \pm S.E.M.). **(C)** Representative images for Alcian
634 blue staining of DMEM + human serum on week 0 (left panel) and week 10 (right panel).

635

636 **Figure 7. Surface roughness, chondrocyte density and volume of *in situ* femoral head**
637 **chondrocytes with time in culture in DMEM + HS. (A)** Surface roughness expressed as the root
638 mean square (RMS) deviation)) in µm at week 0 and week 10, N(n)=3(9), $p=0.2$. **(B)** Cell density
639 (total number of chondrocytes per mm³) at week 0 and week 10, N(n)=3(60), $p=0.22$. **(C)**
640 Chondrocyte volume at week 0 and week 10, N(n)=3(44), $p=0.22$. Broken lines illustrate pairs of data
641 at week 0 and week 10 for each femoral head. (Data shown as mean \pm S.D.).

642

643

644

645

646

647

648 Figure 1.

649

650 (Styczynska-Soczka et al., 2020)

651

652

653

654

655

656

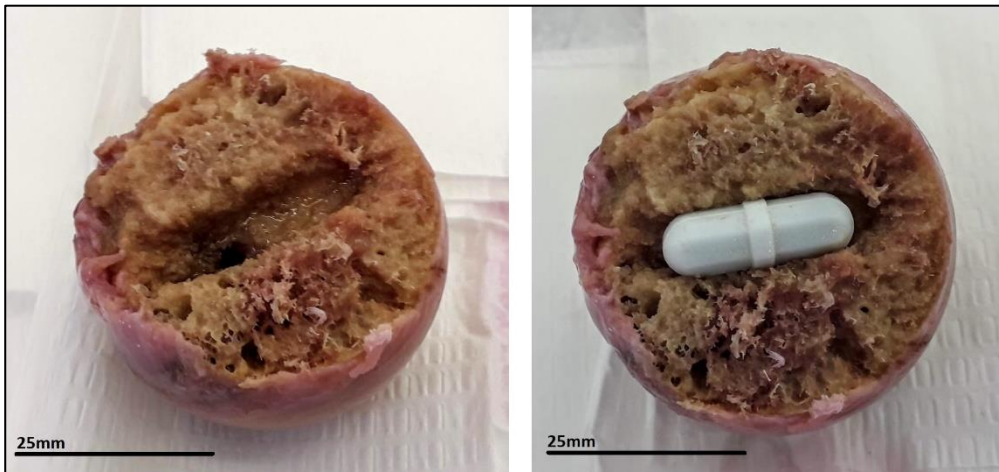
657

658

659

660

661



662

663

664 Figure 2.

665

666 (Styczynska-Soczka et al., 2020)

667

668

669

670

671

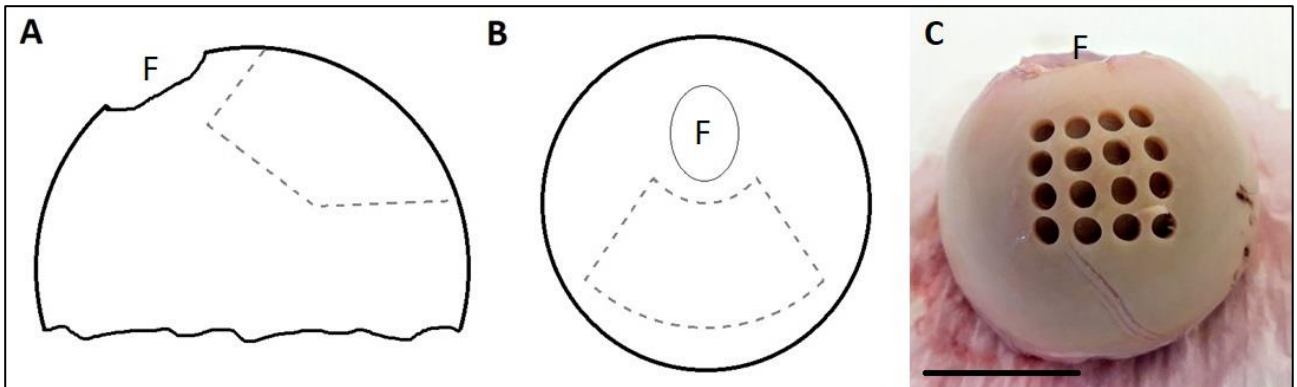
672

673

674

675

676



677

678

679

680

681

682 Figure 3.

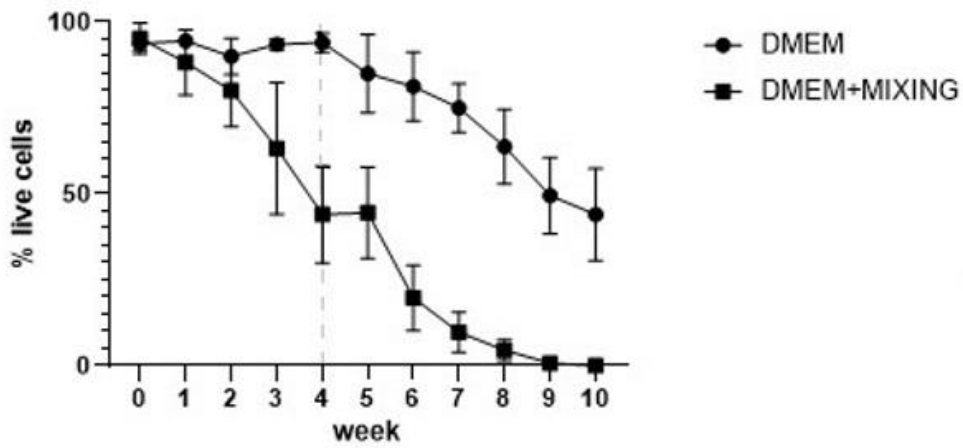
683

684 (Styczynska-Soczka et al., 2020)

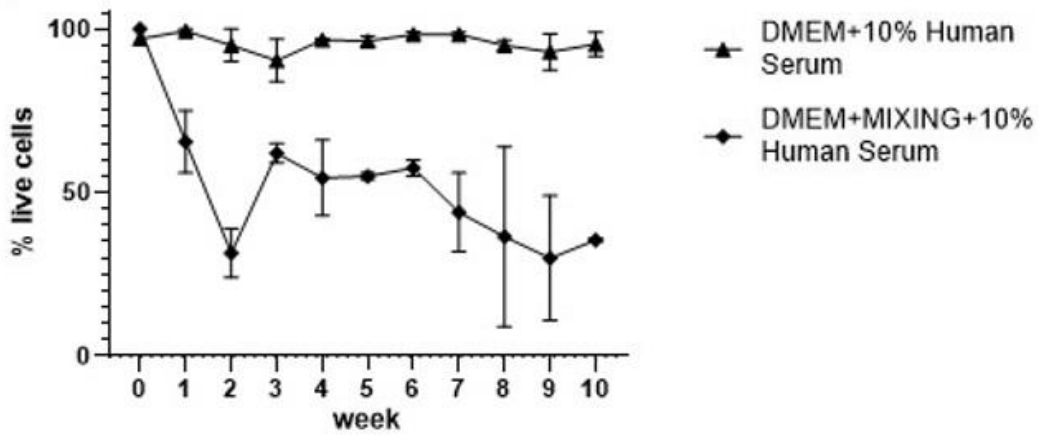
685

686

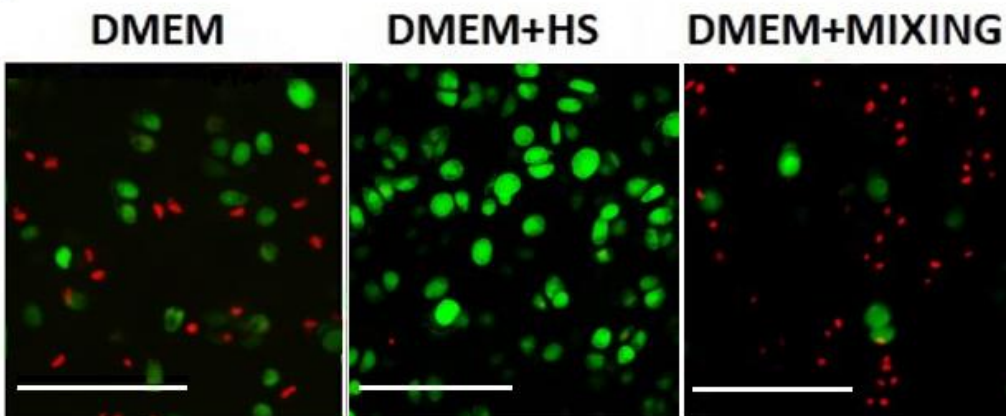
A



B



C



687

688

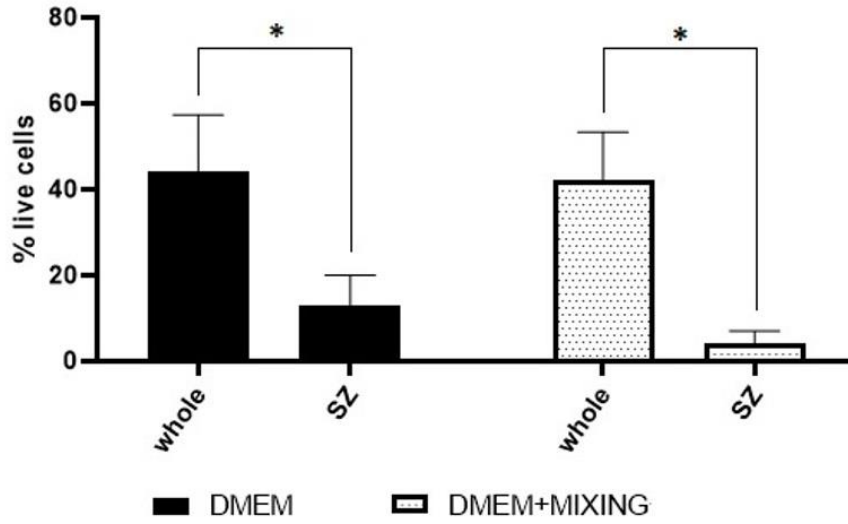
689 Figure 4.

690

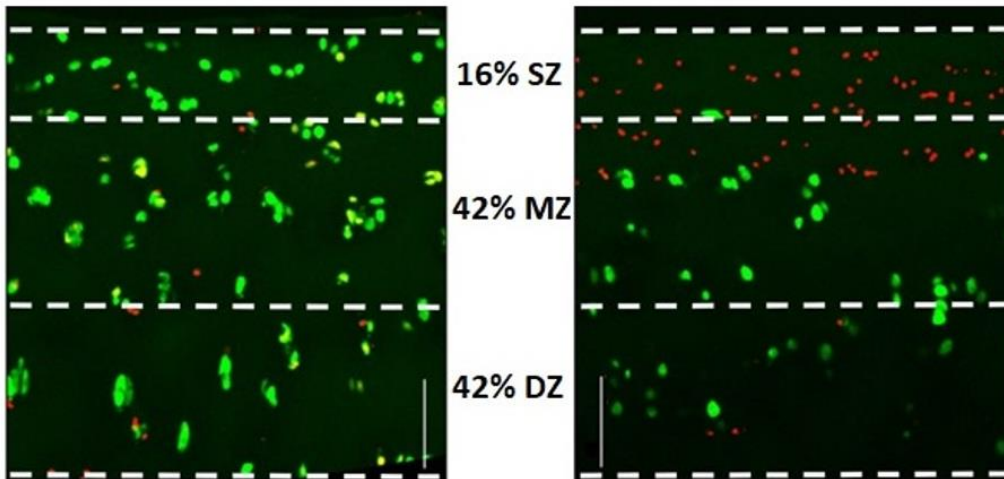
691 (Styczynska-Soczka et al., 2020)

692

A



B



693

694

695

696

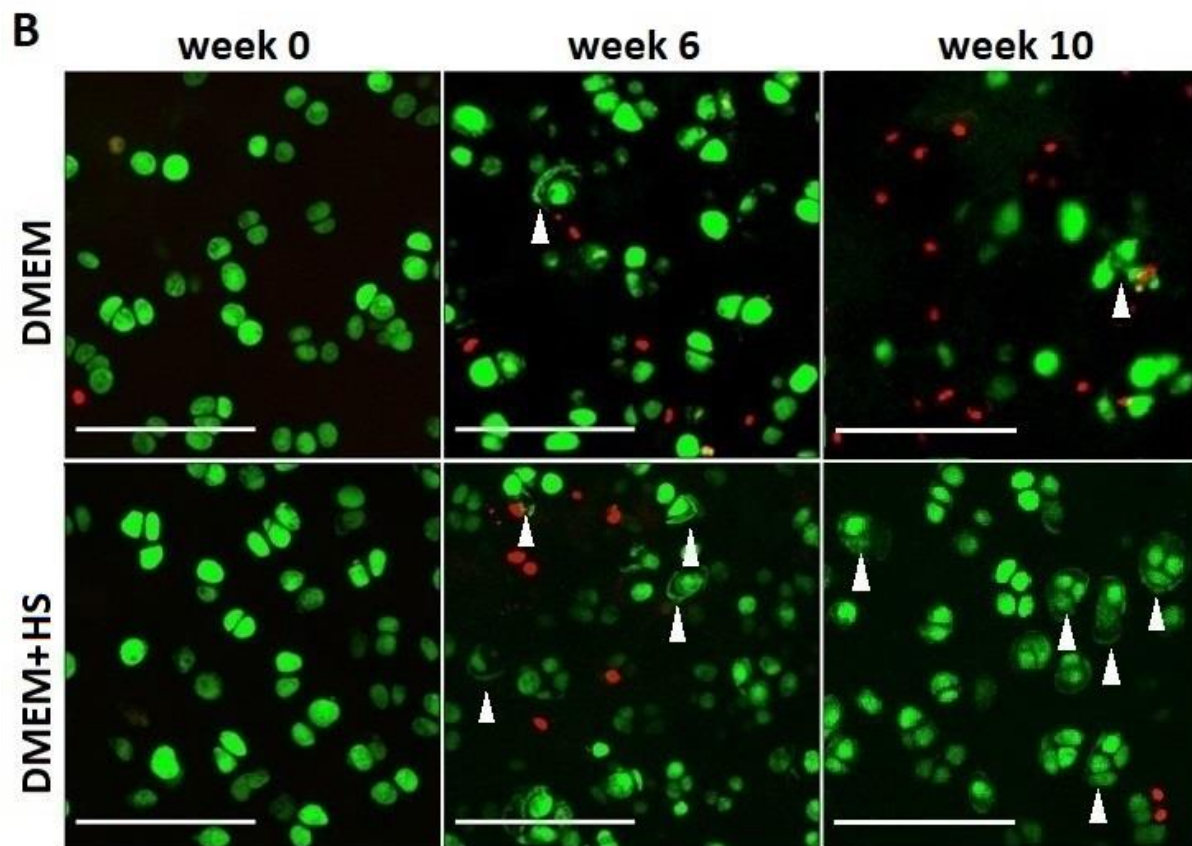
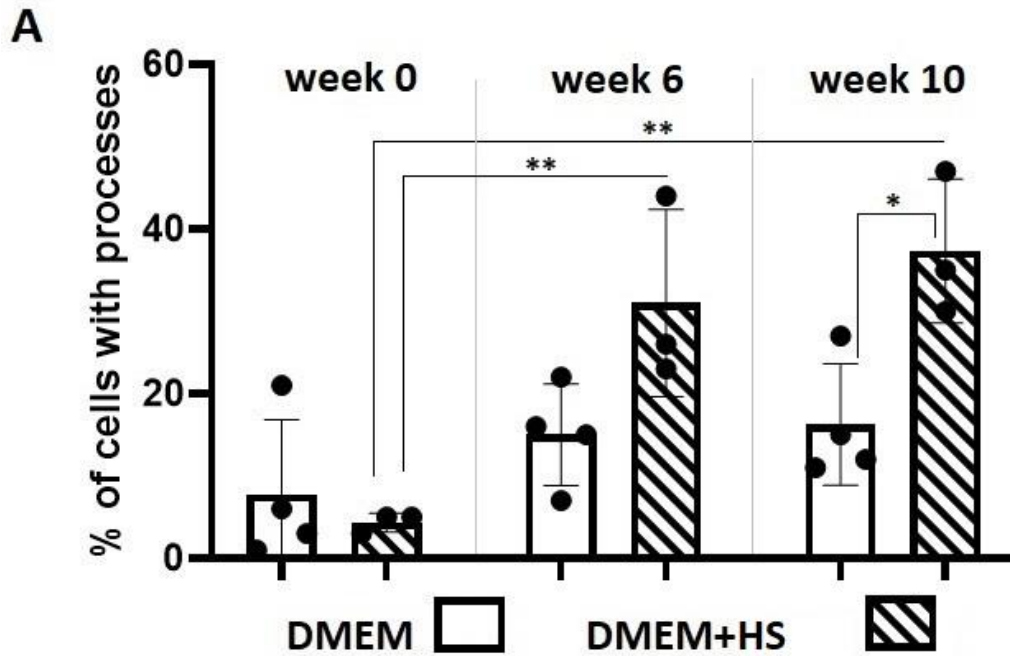
697

698 Figure 5.

699

700 (Styczynska-Soczka et al., 2020)

701



702

703

704

705

706 Figure 6.

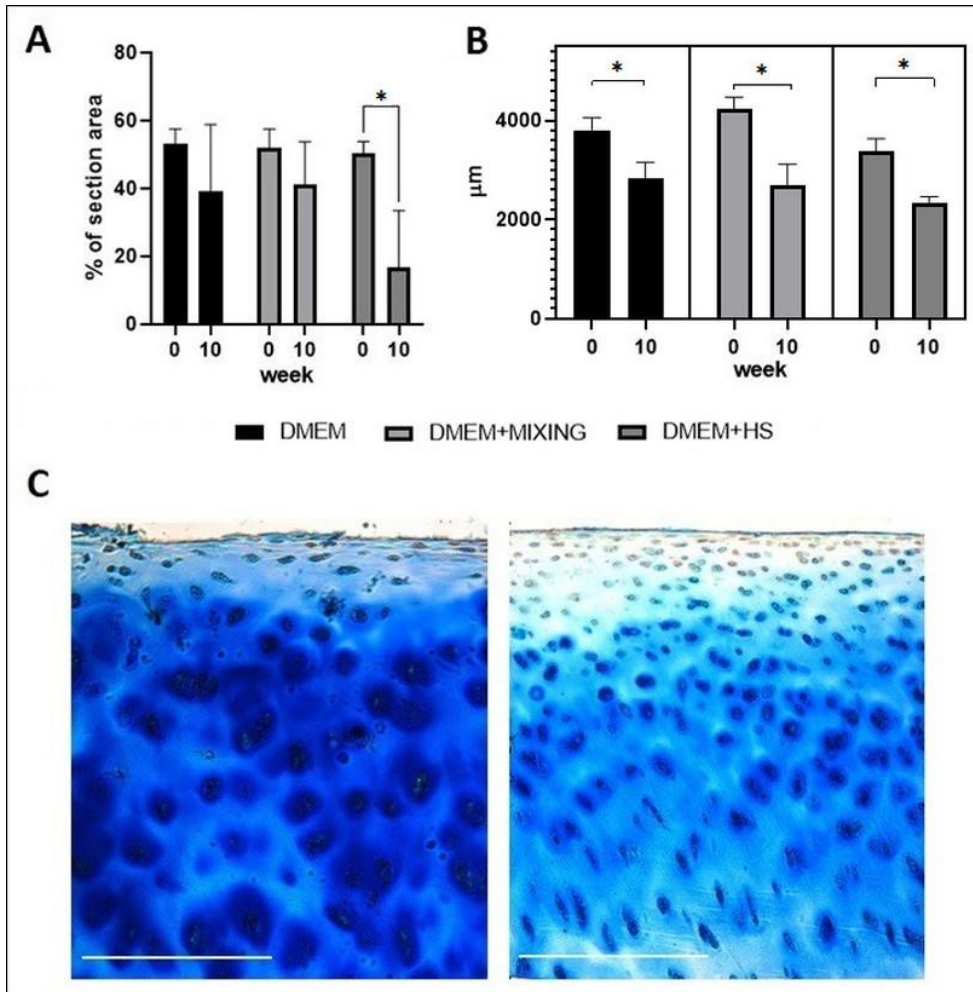
707

708 (Styczynska-Soczka et al., 2020)

709

710

711



712

713

714

715

716

717 Figure 7.

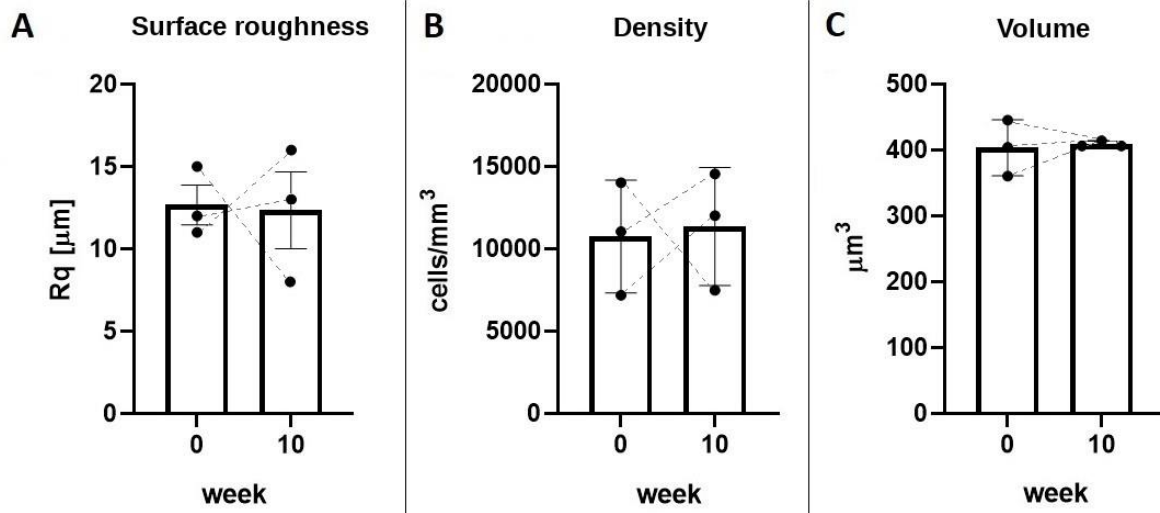
718

719 (Styczynska-Soczka et al., 2020)

720

721

722



723

724

725

726

727

728

729